J|A|C|S
ARTICLES

Published on Web 06/28/2010

Controlled Assembly of Hydrogenase-CdTe Nanocrystal Hybrids for Solar Hydrogen Production

Katherine A. Brown,[†] Smita Dayal,[‡] Xin Ai,[‡] Garry Rumbles,[‡] and Paul W. King*,[†]

Biosciences Center and Chemical and Material Sciences Center, National Renewable Energy Laboratory, Golden, Colorado 80401

Received February 4, 2010; E-mail: paul.king@nrel.gov

Abstract: We present a study of the self-assembly, charge-transfer kinetics, and catalytic properties of hybrid complexes of CdTe nanocrystals (nc-CdTe) and *Clostridium acetobutylicum* [FeFe]-hydrogenase I (H_2ase). Molecular assembly of nc-CdTe and H_2ase was mediated by electrostatic interactions and resulted in stable, enzymatically active complexes. The assembly kinetics was monitored by nc-CdTe photoluminescence (PL) spectroscopy and exhibited first-order Langmuir adsorption behavior. PL was also used to monitor the transfer of photogenerated electrons from nc-CdTe to H_2ase. The extent to which the intramolecular electron transfer (ET) contributed to the relaxation of photoexcited nc-CdTe relative to the intrinsic radiative and nonradiative (heat dissipation and surface trapping) recombination pathways was shown by steady-state PL spectroscopy to be a function of the nc-CdTe/H_2ase molar ratio. When the H_2ase concentration was lower than the nc-CdTe concentration during assembly, the resulting contribution of ET to PL bleaching was enhanced, which resulted in maximal rates of H_2 photoproduction. Photoproduction of H_2 was also a function of the nc-CdTe PL quantum efficiency (PLQE), with higher-PLQE nanocrystals producing higher levels of H_2, suggesting that photogenerated electrons are transferred to H_2ase directly from core nanocrystal states rather than from surface-trap states. The duration of H_2 photoproduction was limited by the stability of nc-CdTe under the reactions conditions. A first approach to optimization with ascorbic acid present as a sacrificial donor resulted in photon-to-H_2 efficiencies of 9% under monochromatic light and 1.8% under AM 1.5 white light. In summary, nc-CdTe and H_2ase spontaneously assemble into complexes that upon illumination transfer photogenerated electrons from core nc-CdTe states to H_2ase, with low H_2ase coverages promoting optimal orientations for intramolecular ET and solar H_2 production.

Introduction

In biology, photosynthesis catalyzes the light-driven oxidation of water into O_2 with production of reduced charge carriers. In phototrophic microbes, these carriers can be electrochemically coupled to catalytic production of H_2 by the enzymatic activity of hydrogenases (H_2ases).[1,2] The overall process of water oxidation to form O_2 and H_2 at pH 7 is summarized by half reactions 1 and 2:

$$H_2O \rightarrow 2H^+ + {}^1/_2O_2 + 2e^- \quad E° = 0.82\ \mathrm{V\ (pH\ 7)} \qquad (1)$$

$$2H^+ + 2e^- \rightarrow H_2 \quad E° = -0.42\ \mathrm{V\ (pH\ 7)} \qquad (2)$$

The overall energetic requirement at pH 0 is 1.23 eV (274 kcal) to produce one mole of H_2 from one mole of water. Development of artificial photosynthesis that can couple the capture of light energy to charge transfer and catalytic H_2 production presents several synthetic challenges, including the need to match absorption spectra (band gaps) and excited-state energy levels, the half-reaction thermodynamic requirements, and formation of molecular assemblies that promote efficient charge transfer and support catalysis.[3−5] One approach to developing synthetic models for achieving reaction 2 involves integrating the H_2ases with photoactive materials and devices.[6] The H_2ases possess catalytic sites with unique organometallic clusters composed of earth-abundant elements (Fe, Ni, S, C, N, and O), operate near or at the thermodynamic potential of the H^+/H_2 couple, and possess large (μs^{-1}) k_{cat} values.[6,7] These enzymes have been incorporated into assemblies with particulate semiconducting materials[8−12] or multi-[13] or single-walled[14,15] carbon nanotubes and employed as as electrocatalysts in photoelectrochemical cells.[16,17]

[†] Biosciences Center.
[‡] Chemical and Material Sciences Center.

(1) Angermayr, S. A.; Hellingwerf, K. J.; Lindblad, P.; Teixeira de Mattos, M. J. *Curr. Opin. Biotechnol.* **2009**, *20*, 257–263.
(2) Ghirardi, M. L.; Dubini, A.; Yu, J. P.; Maness, P. C. *Chem. Soc. Rev.* **2009**, *38*, 52–61.
(3) Bolton, J. R.; Strickler, S. J.; Connolly, J. S. *Nature* **1985**, *316*, 495–500.
(4) Bard, A. J.; Fox, M. A. *Acc. Chem. Res.* **1995**, *28*, 141–145.
(5) Gust, D.; Moore, T. A.; Moore, A. L. *Acc. Chem. Res.* **2009**, *42*, 1890–1898.
(6) Armstrong, F. A.; Belsey, N. A.; Cracknell, J. A.; Goldet, G.; Parkin, A.; Reisner, E.; Vincent, K. A.; Wait, A. F. *Chem. Soc. Rev.* **2009**, *38*, 36–51.
(7) Fontecilla-Camps, J. C.; Amara, P.; Cavazza, C.; Nicolet, Y.; Volbeda, A. *Nature* **2009**, *460*, 814–822.
(8) Cuendet, P.; Grätzel, M.; Pelaprat, M. L. *J. Electroanal. Chem.* **1984**, *181*, 173–185.
(9) Cuendet, P.; Rao, K. K.; Grätzel, M.; Hall, D. *Biochimie* **1986**, *68*, 217–221.
(10) Reisner, E.; Fontecilla-Camps, J. C.; Armstrong, F. A. *Chem. Commun.* **2009**, 550–552.

10.1021/ja101031r

In each of these examples, the interfacial characteristics can have a significant effect on the control of electron transfer (ET) by affecting the orientations, distances, and electronic coupling of the material to the H_2ase. The ET rates must occur on time scales that are competitive with radiative and nonradiative channels in the light absorber material that lead to recombination of free carriers. The relative contributions of these processes can be controlled through the selection and functionalization of the absorber material and the interfacial structure and relative orientations of the absorber and the catalyst. Ideally, the component molecules should assemble in a controlled manner, as in the assembly of the photosynthetic apparatus, in order to acquire multifunctional architectures capable of supporting efficient conversion of light capture into charge transfer and catalysis.

In this report, we investigated the assembly, kinetics, and catalytic properties of hybrids formed from 3-mercaptopropionic acid (MPA)-capped CdTe nanocrystals (nc-CdTe) and *Clostridium acetobutylicum* [FeFe]-hydrogenase (H_2ase). Surface-functionalized nc-CdTe have been characterized[18,19] for both the size and capping-group [e.g., MPA and thioglycolic acid (TGA)] dependence of their photoexcited states.[20−22] There are several examples of proteins adsorbed on nc-CdTe that retain function and activity, forming stable complexes for bioimaging and sensing applications.[23−26] Finally, the radiative recombination rate constants for nc-CdTe are in the μs^{-1} to ns^{-1} range[27] and are compatible with k_{cat} for H_2ases (10^4 s^{-1}). In addition to a high catalytic turnover rate, the *C. acetobutylicum* H_2ase was chosen for investigation on the basis of surface-localized ET [FeS] clusters predicted from structural homology to CpI[28] and the availability of a developed recombinant system for expression and purification.[29]

Materials and Methods

Synthesis and PLQE Measurements of nc-CdTe. CdTe nanocrystals (nc-CdTe) with a particle size of 2.5 nm were synthesized in water using the method of Qian et al.[30] and capped with 3-mercaptopropionic acid (MPA). No further purification was necessary, and all of the samples were stored anaerobically in the dark prior to use. The photoluminescence quantum efficiency (PLQE) was measured using the integrating-sphere method with rhodamine-6G as a reference dye.[31]

[FeFe]-Hydrogenase Expression and Purification. The StrepII-tagged [FeFe]-H_2ase I from *C. acetobutylicum* was expressed and purified from *Escherichia coli* as previously described.[29] Specific activities of H_2ase preparations were measured as the H_2 evolved from sodium dithionite-reduced methyl viologen (MV) (5 mM).[32] The purified H_2ase had specific activities of $\sim$100 (μmol of H_2) mg^{-1} min^{-1}, with concentrations determined by the Bradford assay.[33] Inactive H_2ase samples were prepared by incubating enzyme solutions under a 100% carbon monoxide (CO) atmosphere for 30 min.

Assembly of nc-CdTe-H_2ase Complexes. Mixtures of H_2ase and nc-CdTe solutions for all experiments were prepared in 50 mM Tris-HCl under an anaerobic 4% H_2/96% N_2 atmosphere. The nc-CdTe concentration was determined from the absorbance peak at 514 nm using $\varepsilon = 81\,576\ M^{-1}\ cm^{-1}$ as the extinction coefficient.[34]

Native Polyacrylamide Gel Electrophoresis (PAGE). Mixtures of nc-CdTe-H_2ase complexes were loaded onto native polyacrylamide gels (5 or 6.5%) and electrophoresced at 50 mA under a 4% H_2/96% N_2 atmosphere. Gels were stained in situ for H_2ase activity by soaking in a 10 mM MV solution under the 4% H_2/96% N_2 atmosphere for 5 min. The stained gels were fixed in a 0.1% solution of 2,3,5-triphenyltetrazolium chloride (Sigma) and photographed. Imaging of gels by UV illumination and Coomassie staining was performed under room atmosphere.

Photoluminescence Spectroscopy. Photoluminescence (PL) spectra were collected on a Horiba Jobin Yvon FluoroMax 3 spectrofluorometer with an excitation wavelength of 400 nm. Kinetic PL traces were recorded with an excitation wavelength of 400 nm and an emission wavelength of 548 nm. For kinetic experiments, the nc-CdTe and H_2ase solutions were prepared separately under anaerobic conditions and mixed immediately prior to collection of the PL spectra. The PL spectra of mixtures with active H_2ase (H_2ase^A) were collected under 100% Ar, while those with inactive H_2ase (H_2ase^I) were collected under 100% CO. For equilibrium experiments, the nc-CdTe and H_2ase were mixed under anaerobic conditions, and the PL spectra were collected 45 min after mixing.

Light-Driven H_2 Production. The nc-CdTe-H_2ase samples (300−600 μL in volume) were flushed with 100% Ar for 20 min prior to illumination to remove the residual glovebox H_2. Gas analysis of the sample headspace confirmed the H_2 removal. White-light samples were illuminated for 5 min with a USHIO halogen projector lamp (150 W, 21 V; the spectrum of the lamp is shown in Figure S1 in the Supporting Information) at an intensity of $\sim$AM 3, unless otherwise noted. Light intensities were measured using a light meter (LI-250, LI-COR Biosciences). Headspace H_2 was measured using an Agilent 7890A gas chromatograph (GC) fitted with a 5 Å molecular sieve column (Supelco). Single-wavelength samples were illuminated with a 5 mW 532 nm laser-pointer beam passed through a fiber-optic cable.

(11) Reisner, E.; Powell, D. J.; Cavazza, C.; Fontecilla-Camps, J. C.; Armstrong, F. A. *J. Am. Chem. Soc.* **2009**, *131*, 18457–18466.
(12) Bae, S.; Shim, E.; Yoon, J.; Joo, H. *J. Power Sources* **2008**, *185*, 439–444.
(13) Alonso-Lomillo, M. A.; Rudiger, O.; Maroto-Valiente, A.; Velez, M.; Rodriguez-Ramos, I.; Munoz, F. J.; Fernandez, V. M.; De Lacey, A. L. *Nano Lett.* **2007**, *7*, 1603–1608.
(14) Blackburn, J. L.; Svedruzic, D.; McDonald, T. J.; Kim, Y. H.; King, P. W.; Heben, M. J. *Dalton Trans.* **2008**, 5454–5461.
(15) McDonald, T. J.; Svedruzic, D.; Kim, Y.-H.; Blackburn, J. L.; Zhang, S. B.; King, P. W.; Heben, M. J. *Nano Lett.* **2007**, *7*, 3528–3534.
(16) Bae, B.; Kho, B. K.; Lim, T. H.; Oh, I. H.; Hong, S. A.; Ha, H. Y. *J. Power Sources* **2006**, *158*, 1256–1261.
(17) Hambourger, M.; Gervaldo, M.; Svedruzic, D.; King, P. W.; Gust, D.; Ghirardi, M.; Moore, A. L.; Moore, T. A. *J. Am. Chem. Soc.* **2008**, *130*, 2015–2022.
(18) Gao, M. Y.; Kirstein, S.; Mohwald, H.; Rogach, A. L.; Kornowski, A.; Eychmuller, A.; Weller, H. *J. Phys. Chem. B* **1998**, *102*, 8360–8363.
(19) Li, L.; Qian, H.; Fang, N.; Ren, J. *J. Lumin.* **2006**, *116*, 59–66.
(20) Rajh, T.; Micic, O. I.; Nozik, A. J. *J. Phys. Chem.* **1993**, *97*, 11999–12003.
(21) Zhang, H.; Zhou, Z.; Yang, B.; Gao, M. *J. Phys. Chem. B* **2003**, *107*, 8–13.
(22) Zhang, Y. H.; Zhang, H. S.; Ma, M.; Guo, X. F.; Wang, H. *Appl. Surf. Sci.* **2009**, *255*, 4747–4753.
(23) Gupta, M.; Caniard, A.; Touceda-Varela, A.; Campopiano, D. J.; Mareque-Rivas, J. C. *Bioconjugate Chem.* **2008**, *19*, 1964–1967.
(24) Idowu, M.; Lamprecht, E.; Nyokong, T. *J. Photochem. Photobiol., A* **2008**, *198*, 7–12.
(25) Shen, X. C.; Liou, X. Y.; Ye, L. P.; Liang, H.; Wang, Z. Y. *J. Colloid Interface Sci.* **2007**, *311*, 400–406.
(26) Yuan, J.; Guo, W.; Wang, E. *Anal. Chem.* **2008**, *80*, 1141–1145.
(27) Rogach, A. L.; Franzl, T.; Klar, T. A.; Feldmann, J.; Gaponik, N.; Lesnyak, V.; Shavel, A.; Eychmuller, A.; Rakovich, Y. P.; Donegan, J. F. *J. Phys. Chem., C* **2007**, *111*, 14628–14637.
(28) Peters, J. W. *Curr. Opin. Struct. Biol.* **1999**, *9*, 670–676.
(29) King, P. W.; Posewitz, M. C.; Ghirardi, M. L.; Seibert, M. *J. Bacteriol.* **2006**, *188*, 2163–2172.
(30) Qian, H.; Dong, C.; Weng, J.; Ren, J. *Small* **2006**, *2*, 747–751.
(31) Sun, L.; Bolton, J. R. *J. Phys. Chem.* **1996**, *100*, 4127–4134.
(32) Demuez, M.; Cournac, L.; Guerrini, O.; Soucaille, P.; Girbal, L. *FEMS Microbiol. Lett.* **2007**, *275*, 113–121.
(33) Bradford, M. *Anal. Biochem.* **1976**, *72*, 248–254.
(34) Yu, W. W.; Qu, L.; Guo, W.; Peng, X. *Chem. Mater.* **2004**, *16*, 560.

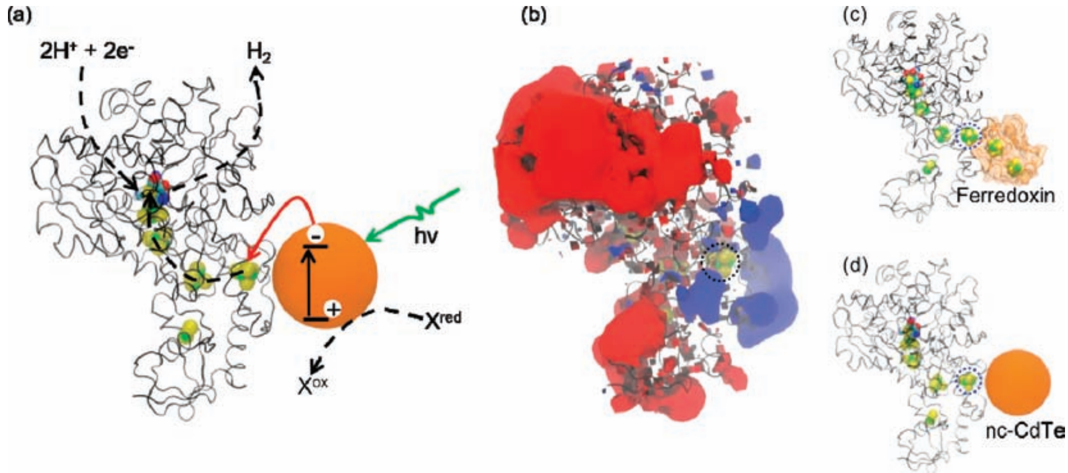

Figure 1. Functional and structural models for nc-CdTe-H_2ase hybrids. (a) The proposed scheme for light-driven H_2 production by the nc-CdTe:H_2ase complex. X, represents a sacrificial hole scavenger. ET [FeS] clusters and the catalytic H cluster are shown in VDW format. Protein structure images were visualized and rendered using the VMD software package.[35,36] Atom colors: yellow, sulfur; green, iron; red, oxygen; blue, nitrogen; cyan, carbon. The H_2ase structures are homology models of *C. acetobutylicum* [FeFe]-H_2ase to *Clostridium pasteurianum* [FeFe]-H_2ase CpI (PDB entry 3C8Y).[37] (b) Electrostatic surface model of H_2ase generated with VMD using VolMap.[35] Regions of positive and negative charge are shown in blue and red, respectively. (c) ClusPro[39–41]-generated docking complex between *C. pasteurianum* ferredoxin (transparent orange, with [4Fe−4S] clusters shown in VDW format) and H_2ase. The ferredoxin [4Fe−4S] cluster is oriented adjacent to the H_2ase distal [4Fe−4S] cluster. (d) Model of a proposed electrostatic complex between MPA-capped nc-CdTe and H_2ase. The nc-CdTe is shown to scale as a 2.5 nm orange sphere.

Effect of pH on H_2ase Activity and Light-Driven H_2 Production. Solutions of 50 mM Tris-HCl with or without 0.05 M ascorbic acid were adjusted to the appropriate pH. Aliquots (μL) of nc-CdTe and H_2ase were diluted 1:100 each in reaction buffer, and H_2 production was monitored by GC under illumination. The effect of pH on H_2ase was measured as H_2 evolution activity from sodium dithionite reduced methyl viologen ($MV^{\cdot+}$, 5 mM). $MV^{\cdot+}$ solutions were adjusted to the appropriate pH and the final $MV^{\cdot+}$ concentration was normalized to an A_{606} value of 0.1 by titrating the amount of NaDTT. A 1 μL aliquot of H_2ase was diluted 1:1000 into 1 mL of $MV^{\cdot+}$ solution in a sealed serum vial, and H_2 production monitored by GC.

Results and Discussion

Assembly of nc-CdTe-H_2ase Complexes. A structural model for the design of a functional nc-CdTe−H_2ase complex for light-driven H_2 production is shown in Figure 1. To achieve directed assembly of this complex in an active and efficient orientation, we first considered the in vivo biochemistry of the enzyme. Intramolecular ET between H_2ase and soluble donor molecules such as ferredoxin (Fd) and flavodoxin is hypothesized to occur via distal [4Fe−4S] or [2Fe−2S] clusters that are positioned close to the enzyme surface.[32] The distal [4Fe−4S] cluster is located near a positively charged surface composed of lysine (p$K_a \approx$ 10.8) and arginine (p$K_a \approx$ 12.5) residues.[28] This positive patch, shown in blue in Figure 1b, is the proposed docking site for Fd.[29] Formation of the ET complex in vivo is partially guided by electrostatic interactions between the negatively charged Fd and the positively charged patch on H_2ase to form the ET complex shown in Figure 1c.[35] We hypothesized that a nanocrystal possessing an overall negative surface charge might mimic Fd, with electrostatic interactions directing the nc-CdTe to dock with H_2ase near the distal [4Fe−4S] cluster (Figure 1d). This would result in a docking complex capable of ET. The use of an MPA capping ligand imparts a negative surface charge on nc-CdTe because the solvent-exposed carboxylic acid moieties are deprotonated in solutions with pH values above the pK_a of 4.3.

To probe the formation of molecular complexes between nc-CdTe and H_2ase^A, the two components were mixed in solution and the resulting complexes separated by native PAGE. Figure 2 shows the stable complexes formed under a range of nc-CdTe-H_2ase^A molar ratios. Illumination under UV light allowed visualization of the nc-CdTe in the complexes, which showed decreasing mobilities with increasing amounts of H_2ase (Figure 2a, lanes 2−5). This effect was due to an increase in the hydrodynamic radius of the nc-CdTe upon adsorption of the H_2ase. The gradual decrease in nc-CdTe mobility with increasing H_2ase suggests that multiple molecules of enzyme can bind to each nc-CdTe. To verify that the adsorbed H_2ase remained active, in situ activity staining was performed. Figure 2b shows that H_2ase was active in each sample and that the mobility of the H_2ase^A increased in the presence of nc-CdTe. The degree of the mobility shift was dependent on the molar ratio (Figure 2b, lanes 2−5) as a result of a decrease in the mass-to-charge ratio of the enzyme upon complexation with negatively charged nc-CdTe. The appearance of a broad molecular-weight band also demonstrated the formation of a variety of molecular complexes, likely to be composed of a range of stoichiometries. Separation of complexes at a higher polyacrylamide concentration (Figure 2c,d) resolved specific banding patterns with molecular weights and distributions that were distinct for each nc-CdTe-H_2ase molar ratio. Overall, the results in Figure 2 demonstrate the assembly of nc-CdTe-H_2ase complexes that are stable in an electric field and nonuniform in molecular composition and in which H_2ase activity is maintained.

Nanocrystal PL is sensitive to changes in both the dielectric environment and the presence of surface adsorbates. Specifically, the adsorption of proteins on nanocrystals causes an increase in the PL intensity due to an increase in nanocrystal PL quantum efficiency (PLQE).[24,25,36,37] The effect of H_2ase adsorption on the nc-CdTe PL can be used to determine the kinetics of

(35) Moulis, J.-M.; Davasse, V. *Biochemistry* **1995**, *34*, 16781–16788.

(36) Mattoussi, H.; Mauro, J. M.; Goldman, E. R.; Anderson, G. P.; Sundar, V. C.; Mikulec, F. V.; Bawendi, M. G. *J. Am. Chem. Soc.* **2000**, *122*, 12142–12150.

(37) Wang, Q.; Kuo, Y.; Wang, Y.; Shin, G.; Ruengruglikit, C.; Huang, Q. *J. Phys. Chem. B* **2006**, *110*, 16860–16866.

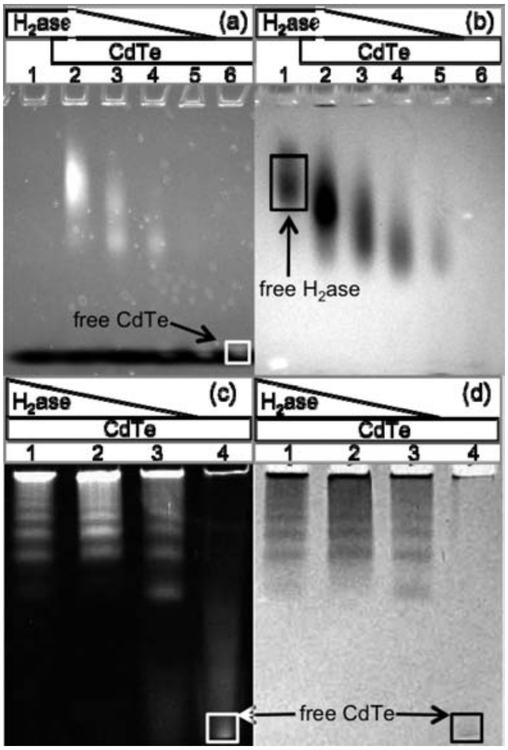

Figure 2. Native PAGE of nc-CdTe-H_2ase^A complexes. The concentration of nc-CdTe was fixed at 15 μM for all lanes containing nc-CdTe, and the amount of H_2ase was adjusted to yield the appropriate molar ratio. Separation of mixtures on 5% gels and photographed for (a) UV illumination and (b) in situ H_2ase activity. Lane 1, 15 μM (20 μg) H_2ase alone; lane 2, 30 μM H_2ase (1:2 nc-CdTe-H_2ase); lane 3, 15 μM H_2ase (1:1 nc-CdTe-H_2ase); lane 4, 7.5 μM H_2ase (2:1 nc-CdTe-H_2ase); lane 5, 3.75 μM H_2ase (4:1 nc-CdTe-H_2ase); lane 6, 15 μM nc-CdTe alone. (c, d) Separation of mixtures on 6.5% gels and photographed for (c) UV illumination and (d) Coomassie stain. Lane 1, 30 μM H_2ase (1:2 nc-CdTe-H_2ase); lane 2, 15 μM H_2ase (1:1 nc-CdTe-H_2ase); lane 3, 7.5 μM H_2ase (2:1 nc-CdTe-H_2ase); lane 4, 15 μM nc-CdTe alone.

complex formation. Figure 3a shows changes in the PL emission response of 0.37 μM nc-CdTe over time after addition of various concentrations of H_2ase^I. The change in PL intensity was dependent on the amount of H_2ase^I added, with higher amounts of enzyme yielding larger PL increases. Modeling of these results using the kinetic first-order Langmuir isotherm equation (eq 3) allowed calculation of the observed rate constant (k_{obs}) for adsorption of H_2ase^I to nc-CdTe.[38,39]

$$\Delta I = \Delta I_{max}(1 - e^{-k_{obs}t}) \tag{3}$$

To obtain eq 3, the standard Langmuir equation was modified under the assumption that the change in the nc-CdTe PL intensity (ΔI) is proportional to the number of molecules adsorbed on each nanocrystal.[40] The value of k_{obs} can be used to calculate the rate constants for the adsorption (k_a) and desorption (k_d) of H_2ase on the nanocrystal surface using the expression $k_{obs} = k_a[H_2ase] + k_d$ (Figure S2 and Table S1 in the Supporting Information). The ratio k_a/k_d is equal to the Langmuir equilibrium constant (K_L), which can be used to calculate the free energy of H_2ase^I adsorption using the relation

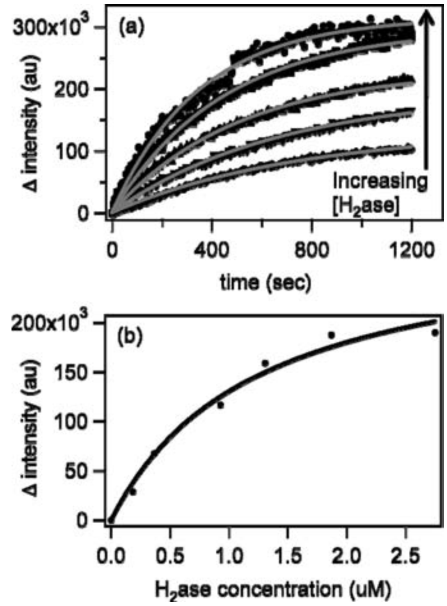

Figure 3. Response of nc-CdTe PL intensity to H_2ase^I adsorption. (a) Time courses of nc-CdTe (0.37 μM) PL responses to the addition of increasing concentrations of H_2ase^I (0.37, 0.75, 1.87, 2.80, and 3.74 μM). Solid gray lines represent fits to the first-order adsorption equation (eq 3). (b) PL of equilibrated nc-CdTe-H_2ase^I mixtures taken 45 min after the addition of the specified amount of H_2ase^I to 0.1 μM nc-CdTe. The solid line represents the fit to the Langmuir isotherm (eq 4).

Table 1. Kinetic and Thermodynamic Parameters for H_2ase^I Adsorption on nc-CdTe

equation	k_a (L mol^{-1} s^{-1})	k_d (s^{-1})	K_L (μM^{-1})	ΔG_{ads} (kcal mol^{-1})
3	428 ± 72	$(1.2 \pm 0.2) \times 10^{-3}$	0.37 ± 0.10	-7.6 ± 0.2
4	–	–	0.81 ± 0.36	-8.0 ± 0.3

$\Delta G_{ads} = -RT \ln K_L$.[38,39] The calculated values of these parameters are listed in Table 1.

The change in PL intensity at equilibrium as a function of H_2ase^I concentration is shown in Figure 3b. Steady-state absorption can be modeled using the Langmuir isotherm (eq 4), here modified under the same assumption as above ($\Delta I \propto$ coverage). The values of K_L and ΔG_{ads} obtained from the fit to eq 4 are also listed in Table 1.

$$\Delta I = \frac{\Delta I_{max} K_L[H_2ase]}{1 + K_L[H_2ase]} \tag{4}$$

On the basis of the calculated parameters obtained from the kinetic and equilibrium data, we can compare the adsorption behavior of the nc-CdTe-H_2ase^I system to that of other nanocrystal systems. Comparison of the ΔG_{ads} values shows that the nc-CdTe-H_2ase systems fall in the regime between strong interactions that result in the formation of a true covalent bond[41] and weak transient binding that results in labile associations.[42] This energy regime is consistent with the formation of a stable complex partially controlled by electrostatics.

Electron Transfer in the nc-CdTe-H_2ase Complexes. It is important to note that the results in Figure 3 represent the PL

(38) Karpovich, D. S.; Blanchard, G. J. *Langmuir* **1994**, *10*, 3315–3322.
(39) Park, J. J.; Lacerda, S. H. D. P.; Stanley, S. K.; Vogel, B. M.; Kim, S.; Douglas, J. F.; Raghavan, D.; Karim, A. *Langmuir* **2009**, *25*, 443–450.
(40) Bullen, C.; Mulvaney, P. *Langmuir* **2006**, *22*, 3007–3013.
(41) Wang, H.; Wang, C.; Lei, C.; Wu, Z.; Shen, G.; Yu, R. *Anal. Bioanal. Chem.* **2003**, *377*, 632–638.
(42) Aslam, M.; Mulla, I. S.; Vijayamohanan, K. *Langmuir* **2001**, *17*, 7487–7493.

intensity change for nc-CdTe complexed with catalytically inactive H_2ase. This was necessary in order to characterize only the surface passivation effects of H_2ase adsorption on the nc-CdTe PL spectra. The formulas for the PLQE of nc-CdTe alone and complexed with either H_2ase^I or H_2ase^A are given in eqs 5−7, respectively:

$$\mathrm{PLQE}_{\mathrm{CdTe}} = \frac{k_{\mathrm{RR}}}{k_{\mathrm{RR}} + k_{\mathrm{NR}} + k_{\mathrm{ST}}[\mathrm{T}]} \tag{5}$$

$$\mathrm{PLQE}_{(\mathrm{I})} = \frac{k_{\mathrm{RR}}}{k_{\mathrm{RR}} + k_{\mathrm{NR}} + k_{\mathrm{ST}}[\mathrm{T}']} \tag{6}$$

$$\mathrm{PLQE}_{(\mathrm{A})} = \frac{k_{\mathrm{RR}}}{k_{\mathrm{RR}} + k_{\mathrm{NR}} + k_{\mathrm{ST}}[\mathrm{T}'] + k_{\mathrm{ET}}[\mathrm{H_2ase}]} \tag{7}$$

in which k_{RR} is the rate constant for radiative recombination, k_{NR} is the rate constant for charge relaxation in which the energy is dissipated as heat, k_{ET} is the rate constant for ET between adsorbed H_2ase^A and nc-CdTe, k_{ST} is the rate constant for surface trapping, [T] is the concentration of surface traps on nc-CdTe alone, and [T′] is the concentration of surface traps when H_2ase is adsorbed. The PL increase shown in Figure 3 is the result of the passivation of nc-CdTe surface traps by H_2ase^I (i.e., [T′] < [T]). Adsorption of catalytically active H_2ase^A also passivates surface traps but in addition creates an ET pathway from nc-CdTe to the enzyme with a rate constant k_{ET}. These two pathways should have opposite effects on the nc-CdTe PL, with the overall change in PL intensity upon adsorption of H_2ase^A being the sum of the k_{ET} component and the passivation effect observed for adsorption of H_2ase^I. This hypothesis is supported by the results shown in Figure 4a: a 1:10 nc-CdTe-H_2ase^I mixture resulted in a 49.6% increase in the nc-CdTe PL relative to that for nanocrystals alone (Figure 4a, black line vs dark-gray line), while the same concentration of H_2ase^A resulted in an increase of only 12.8% (Figure 4a, light-gray line). A control sample of nc-CdTe and buffer showed no change in PL intensity with time (Figure 4a, dark-gray line).

The nc-CdTe PL response also reveals a qualitative assessment of the events during nc-CdTe-H_2ase complex formation. In the 1:10 nc-CdTe-H_2ase^I sample (Figure 4a, black line), there was a rapid increase in the PL immediately following enzyme addition, which was likely due to the formation of electrostatically mediated encounter complexes similar to those observed during formation of biological ET complexes[43] and the passivation of surface-trap states in the nc-CdTe. The PL continued to increase, but at a slowly diminishing rate, until the system reached equilibrium after 10−15 min. This slower increase may represent the H_2ase adopting the most energetically stable orientation within the complex. Addition of H_2ase^A at a 1:10 ratio also resulted in an immediate increase in nc-CdTe PL, but the signal soon leveled off and eventually declined. We hypothesize that the initial rapid increase with H_2ase^A was due to formation of the same encounter complexes and surface-trapping effects as with H_2ase^I. However, once nc-CdTe-H_2ase^A complexes had formed, ET from nc-CdTe to H_2ase^A resulted in an attenuation of PL intensity. This effect was more pronounced at low nc-CdTe-H_2ase^A ratios, which appear to favor a more rapid formation of ET-competent complexes. Figure 4b shows the PL response of nc-CdTe with H_2ase^I or H_2ase^A at a 1:1 ratio. The PL response with H_2ase^I was similar in shape to that observed for the 1:10 ratio. In contrast, H_2ase^A added at a 1:1 ratio showed that ET dominated the PL signal earlier than at a 1:10 ratio. This dependence of the PL response on H_2ase^A concentration suggests that formation of an efficient ET complex

(43) Tang, C.; Iwahara, J.; Clore, G. M. *Nature* **2006**, *444*, 383–386.

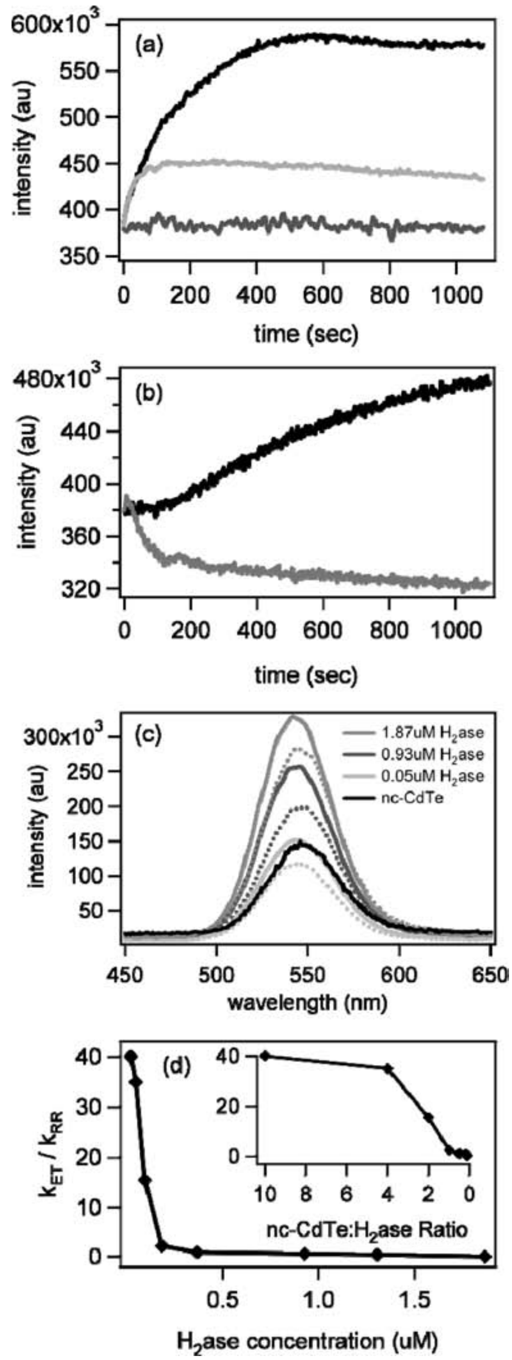

Figure 4. Effect of H_2ase concentration on nc-CdTe PL and steady-state ET kinetics of nc-CdTe-H_2ase mixtures. (a) PL intensity change for nc-CdTe (0.37 μM) with time following addition of a 10-fold (3.74 μM) molar excess of either H_2ase^I (black) or H_2ase^A (light gray). A sample with buffer alone (dark gray) is also shown as a control. (b) PL intensity change for nc-CdTe (0.37 μM) with time following addition of an equimolar amount (0.37 μM) of H_2ase^I (black) or H_2ase^A (light gray). (c) PL spectra of nc-CdTe (0.1 μM) at equilibrium for several concentrations of either H_2ase^I (solid lines) or H_2ase^A (dotted lines). Spectra were collected 45 min after H_2ase addition. (d) Relative rate constants for electron transfer (k_{ET}) and radiative recombination (k_{RR}) in nc-CdTe-H_2ase^A complexes (0.1 μM nc-CdTe) as a function of either H_2ase concentration or (inset) molar ratio. The data in (c) represent a subset of the data used to calculate k_{ET}/k_{RR} values shown in (d).

is affected by the number of molecules that adsorb on the nanocrystal surface, with lower H_2ase^A concentrations facilitating more rapid formation of ET-competent complexes.

To quantify more clearly the effect of the nc-CdTe-H_2ase^A ratio on ET, we compared the PL responses of nc-CdTe to the adsorption of H_2ase^I and H_2ase^A for a range of concentrations (Figure 4c). The decrease in PL intensity with H_2ase^A relative to H_2ase^I was detected over a wide range of H_2ase concentrations, including samples where H_2ase^I had a negligible effect on the PL (Figure 4c, light-gray lines, 1:10 nc-CdTe-H_2ase). Using the definitions of PLQE in eqs 6 and 7, we derived the expression for the ratio k_{ET}/k_{RR} shown in eq 8:

$$\frac{k_{ET}}{k_{RR}} = \left(\frac{\text{Area}_{(I)}}{\text{Area}_{(A)}} - 1\right)\frac{1}{[\text{H}_2\text{ase}]\cdot\text{PLQE}_{[\text{H}_2\text{ase}]}} \qquad (8)$$

where $PLQE_{H_2ase}$ is the PLQE of nc-CdTe at a given H_2ase concentration and $Area_{(I)}$ and $Area_{(A)}$ are the nc-CdTe PL peak areas at specific concentrations of H_2ase^I and H_2ase^A, respectively (for the full derivation, see the Supporting Information). The value of k_{ET}/k_{RR} was calculated for each H_2ase concentration using eq 8, and the results are plotted in Figure 4d. The value of k_{RR} is not affected by enzyme adsorption,[27] so the change in k_{ET}/k_{RR} is due to changes in the contribution of ET to the PL for each nc-CdTe-H_2ase^A mixture. Each ratio yields a distribution of complexes (Figure 2c), each of which has a unique average number of H_2ase molecules per nanocrystal. The calculated values of k_{ET}/k_{RR} are a relative measure of the capacities of specific distributions of nc-CdTe-H_2ase^A complexes to participate in ET. Ratios that result in a statistical bias toward low coverages of H_2ase (2:1, 4:1, and 10:1 nc-CdTe-H_2ase; Figure 4d inset) show dramatically higher values of k_{ET}/k_{RR}, suggesting that ET is a more efficient process in complexes with fewer H_2ase molecules per nc-CdTe.

This result is surprising, since on the basis of eq 7 we would expect a higher surface coverage of H_2ase^A to lead to a greater contribution of ET, as is seen with small-molecule electron acceptors.[44] We considered two possible explanations: (1) that the high level of surface passivation at high H_2ase^A coverage is somehow detrimental to ET and/or (2) that high coverages of H_2ase might result in complexes where a smaller fraction of H_2ase^A molecules have the correct orientation to contribute to ET. If ET between nc-CdTe and H_2ase^A occurs via surface-trap states (T), then raising the enzyme coverage, which would increase passivation of traps and reduce [T], should result in reduced ET and a lower contribution of k_{ET} to the PL signal. Alternatively, if the binding of multiple H_2ase^A molecules causes crowding on the nc-CdTe surface, the complexes that are formed at high enzyme ratios may have orientations that are not optimal for ET. An increase in the distance between the nanocrystal surface and the intramolecular transport chain of the H_2ase would decrease the contribution of k_{ET}, so lower coverages of H_2ase should result in better ET.

We investigated the effect of the inherent PLQE value of the nc-CdTe on the overall H_2 production capacity of the hybrid complexes under illumination in order to determine which of the above hypotheses is correct. We predicted that the H_2 production rates should be proportional to k_{ET}/k_{RR} for a given H_2ase^A concentration. For a constant size of nc-CdTe, the PLQE is largely a function of the number of trap states,[27] where PLQE $\propto$ 1/[T] (see eq 5). If electrons from nc-CdTe are transferred to H_2ase^A via trap states, then nc-CdTe with higher [T] and lower PLQE should contribute to higher levels of H_2. However, if the electrons are transferred directly from the nc-CdTe conduction band, nc-CdTe with low [T] and a high PLQE should contribute to higher levels of H_2. Figure 5 shows the H_2 production by a 2:1 nc-CdTe-H_2ase^A mixture prepared from two separate syntheses of 2.5 nm CdTe nanocrystals. The high-PLQE (17.5%) nc-CdTe led to production of ~1.7 times more H_2 after 5 min of illumination than did the low-PLQE (4%) sample. These results lead us to conclude that the electrons transferred to H_2ase^A are not transferred from trap states, which means that passivation is not responsible for the low k_{ET} values at higher H_2ase^A coverages. We therefore conclude that a high H_2ase^A concentration leads to diminished k_{ET}/k_{RR} and low H_2 production rates as a result of crowding on the nanocrystal surface and formation of nonoptimal ET complexes.

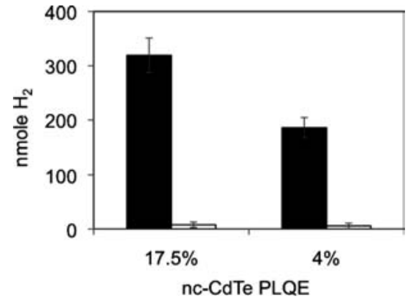

Figure 5. Dependence of H_2 production on the nc-CdTe PLQE. A 2:1 molar mixture of nc-CdTe-H_2ase^A (0.50 μM nc-CdTe) was either illuminated (black bars) or kept in the dark (white bars) for a period of 5 min, and the amount of H_2 produced was measured by gas chromatography. All reactions were performed in a solution of 0.5 M ascorbic acid (pH 4.75).

Optimization of H_2 Production. The photoproduction of H_2 shown in Figure 5 was accomplished in the presence of ascorbic acid, which acted as a sacrificial donor to maintain charge neutrality by quenching the hole remaining in the nc-CdTe after ET. Ascorbic acid is an effective hole scavenger for nc-CdTe for several reasons. The equilibrium redox potential of ascorbic acid[45] is sufficiently negative to reduce photogenerated holes in nc-CdTe, but it is too positive to directly reduce H_2ase^A and cannot contribute to chemically driven H_2 production. In addition, ascorbic acid oxidation is a two-electron process, complementing the two-electron process of H_2 production by H_2ase. Table 2 shows the H_2 production activity of a 1:1 nc-CdTe-H_2ase^A (0.50 μM) solution containing 50 mM ascorbic acid and buffered over a range of pH values. The ascorbic acid affects the solution pH, and it was necessary to adjust for this effect prior to addition of the nc-CdTe and H_2ase^A. The solution pH had a strong effect on rates of light-driven H_2 production by nc-CdTe-H_2ase complexes but had less of an effect on the activity of H_2ase alone (Table 2). For the nc-CdTe-H_2ase, a sharp maximum was observed at a pH range of 4.5–4.75, which was an ~100-fold higher rate than that observed at pH 7. In contrast, H_2ase H_2 evolution activity peaked at pH 7, which was only ~2-fold higher than the activity observed at pH 4.75. The effects of pH are complex and include a 59 mV per pH unit change in the H^+/H_2 (H_2ase) reduction potential, changes in the stabilities of the nc-CdTe MPA capping group and the ascorbic acid, and modulation of complex formation through electrostatics (discussed below). For example, at near neutral pH dehydroascor-

(44) Dimitrijevic, N. M.; Savic, D.; Micic, O. I.; Nozik, A. J. *J. Phys. Chem.* **1984**, *88*, 4278–4283.

(45) Davenport, H.; Jeffreys, C.; Warner, R. *J. Biol. Chem.* **1937**, *117*, 237–279.

Table 2. Effect of Solution pH on H_2 Production by a 1:1 nc-CdTe-H_2ase^A (0.25 μM) Molar Mixture in 0.05 M Ascorbic Acid and on H_2ase Activity

buffer pH[a]	nc-CdTe-H_2ase H_2 production[b] (μmol H_2 mg^{-1} H_2ase min^{-1})	H_2ase activity[c] (μmol H_2 mg^{-1} H_2ase min^{-1})
4	0.79 ± 0.12	26.4 ± 1.8
4.25	1.06 ± 0.31	46.7 ± 3.9
4.5	1.85 ± 0.22	46.2 ± 2.1
4.75	1.94 ± 0.30	49.1 ± 5.3
5	0.64 ± 0.25	43.1 ± 5.1
5.5	0.069 ± 0.013	60.8 ± 8.6
6	0.038 ± 0.007	57.2 ± 5.2
6.5	0.031 ± 0.004	79.6 ± 13.1
7	0.020 ± 0.003	107.0 ± 14.9

[a] Buffer composition: 50 mM Tris-HCl, 5 mM NaCl, 5% glycerol. [b] Measured as total H_2 after 5 min illumination. [c] Measured as rates in 5 mM MV.

bate becomes unstable,[45] which shifts the equilibrium of the redox reaction and reduces the ability of ascorbic acid to function as a sacrificial donor. However, at pH ≤ 6 the MPA ligands begin to dissociate from the nc-CdTe surface[46] causing precipitation. Thus, the nc-CdTe and ascorbic acid are most stable in acidic buffers, whereas H_2ase activity as shown in Table 2 is only minimally affected by pH in the range that was tested. We attribute the observed pH optimum for nc-CdTe-H_2ase light-driven H_2 production to a balance of these competing effects and, based on the data in Table 2, are optimal at pH 4.75. Therefore, this pH value was used for all of the subsequent light-driven H_2 production experiments.

Figure 6a shows the production of H_2 over time for a 1:1 nc-CdTe-H_2ase^A (0.25 μM) mixture in 0.1 M ascorbic acid at pH 4.75 under illumination and in the dark. No significant H_2 production was seen in samples kept in the dark, indicating that light is necessary to provide the electrochemical driving force for ET and the catalytic activity of H_2ase. The rate of H_2 production was linear during the first 5 min of illumination (inset) and then declined with increasing illumination time. This result suggests that H_2 production is continuous as long as ascorbic acid is in excess. After 5 min of illumination, a total of ~70 nmol of H_2 was produced. Since these solutions contained 150 pmol of nc-CdTe (600 μL of 0.25 μM nc-CdTe) and two electrons are required for each molecule of H_2 produced, each nc-CdTe transferred >900 electrons to the H_2ase. This result confirms that the nc-CdTe ground state is regenerated through hole scavenging by ascorbic acid and that hole scavenging is an essential component of efficient H_2 production. The effect of the ascorbic acid concentration on H_2 production is shown in Figure 6b. In samples without ascorbic acid, only a small amount of H_2 was produced. There was a significant increase in H_2 production with increasing ascorbic acid concentration up to 0.2 M. Additional increases in ascorbic acid concentration led to more modest increases in H_2 production. As the H_2 production did not show a peak but changed minimally above 0.5 M ascorbic acid, we selected this concentration and pH 4.75 as the standard reaction conditions for further experiments.

The photoproduction of H_2 shown in Figures 5 and 6 demonstrates that the nc-CdTe-H_2ase^A complexes are capable of light-driven enzyme catalysis. This suggests that an electrostatically guided orientation illustrated in Figure 1d is reasonable. In order to further elucidate the role of electrostatics on complex formation and stability, the effect of buffer ionic strength on H_2 production was tested. High salt concentrations increase the

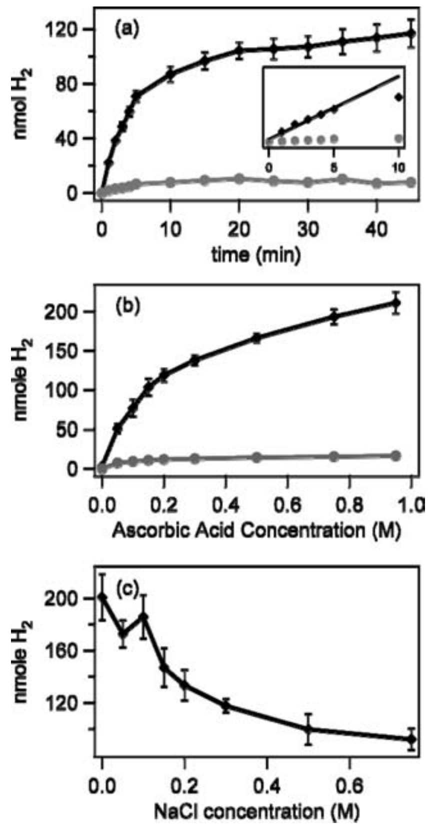

Figure 6. Effect of ascorbic acid concentration and ionic strength on H_2 production by a 1:1 mixture of nc-CdTe-H_2ase^A (0.25 μM). (a) Rate of H_2 production under illumination (black ◆) or in the dark (gray ●) in 0.1 M ascorbic acid (pH 4.75). (b) Total H_2 production after 5 min by solutions with varying ascorbic acid concentrations at pH 4.75. Reactions were illuminated (black ◆) or kept in the dark (gray ●). (c) Total H_2 production after 5 min in 0.5 M ascorbic acid at various NaCl concentrations. The reactions were illuminated and the dark signals subtracted.

ionic strength of the solution, decrease the Debye length, and screen out electrostatic interactions. Figure 6c shows the effect of increasing NaCl concentration on light-driven H_2 production by a 1:1 nc-CdTe-H_2ase^A (0.25 μM) mixture in 0.5 M ascorbic acid. The NaCl was added prior to the addition of the H_2ase in order to assess the effect of ionic strength on complex formation. In solutions with low ionic strength (≤0.1 M), H_2 production was comparable to that in solutions without added salt, whereas subsequent increases in NaCl concentration resulted in significant decreases in H_2 production levels. At 0.75 M NaCl, the H_2 production was ~50% of that seen for solutions without NaCl. We attribute this result to less efficient complex formation and decreased ET. The effect of increasing ionic strength is similar to the effect on H_2 production rates by Fd−H_2ase complexes in vitro,[36] though a comparison of the two systems shows that a higher ionic strength is required to disrupt the nc-CdTe-H_2ase^A charge-transfer complexes. This is not surprising since nc-CdTe has a substantially higher charge density than Fd and possesses empty valence states (surface traps) that may contribute to strong adsorption by the surface functional groups of H_2ase. What is clear from these results is that electrostatic forces make an important contribution to nc-CdTe-H_2ase^A complex formation, consistent with the model shown in Figure 1b.

Given the effect of the nc-CdTe-H_2ase^A ratio on the complex distribution and ET rates, it was likely that the photocatalytic H_2 production would depend on this ratio. Figure 7a shows the H_2 production at a fixed H_2ase concentration (0.5 μM) with

(46) Aldana, J.; Lavelle, N.; Wang, Y. J.; Peng, X. G. *J. Am. Chem. Soc.* **2005**, *127*, 2496–2504.

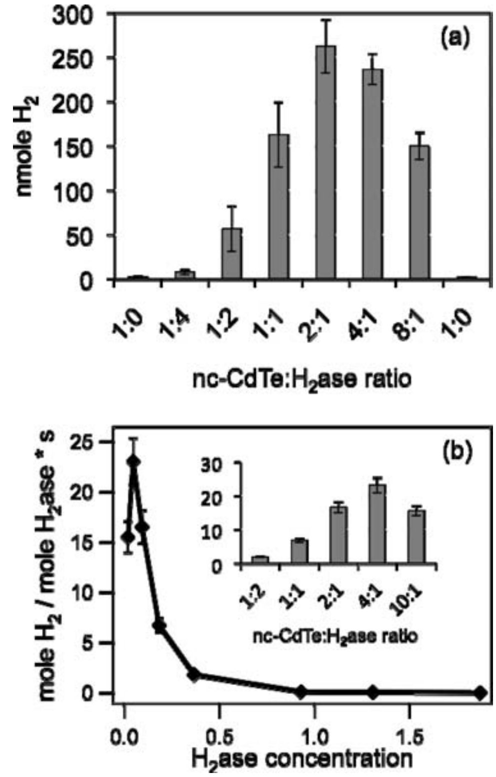

Figure 7. Effect of H_2ase concentration on light-driven H_2 production by nc-CdTe-H_2ase^A complexes. (a) Amount (nmol) of H_2 produced by 0.5 μM H_2ase^A mixed with various concentrations of nc-CdTe to achieve molar mixtures of the given ratios (0.5 M ascorbic acid, pH 4.75) after 5 min of illumination (dark signal subtracted). (b) Enzyme turnover [(mol of H_2) (mol of H_2ase)$^{-1}$ s^{-1}] in a solution of fixed nc-CdTe concentration (0.1 μM) as a function of either H_2ase^A concentration or (inset) nc-CdTe-H_2ase molar ratio in 0.5 M ascorbic acid (pH 4.75).

increasing nc-CdTe concentration. The levels of H_2 production were highest in samples with ratios that favor fewer H_2ase per nc-CdTe, consistent with the concentration dependence of k_{ET}/k_{RR} shown in Figure 4d. In order to directly compare the H_2 production to the results of the k_{ET}/k_{RR} calculations, samples with identical nc-CdTe and H_2ase^A concentrations were illuminated in 0.5 M ascorbic acid (Figure 7b). The H_2 production rate is calculated as the enzyme turnover number (TON) rather than moles of H_2 in order to normalize for differences in H_2ase^A concentration. The data show a trend favoring low H_2ase^A concentrations that is similar to the k_{ET}/k_{RR} results in Figure 4d. Together these two results confirm that optimal complex assembly for light-driven H_2 production occurs at low H_2ase^A concentrations relative to nc-CdTe.

To evaluate the photon-to-H_2 efficiency of nc-CdTe-H_2ase^A complexes, a 2:1 nc-CdTe-H_2ase^A molar mixture (0.5 μM nc-CdTe) in 0.50 M ascorbic acid buffer was prepared, and the H_2 production was monitored under illumination with a monochromatic light source (532 nm). The average number of photons absorbed by the nc-CdTe (N_0) is given by eq 9:[47,48]

$$N_0 = J(0)\frac{1 - e^{-\mathrm{OD}\ln 10}}{cL} \qquad (9)$$

where $J(0)$ is the incident photon flux, OD is the optical density of the solution at 532 nm, c is the nc-CdTe concentration (in mol mol^{-3}), and L is the optical path length (in m). In excess ascorbic acid, the theoretical maximum amount of H_2 produced during 5 min of illumination was calculated to be 114 nmol using the measured $J(0)$ of 352 μmol of photons s^{-1} m^{-2} and a total of 150 pmol of nc-CdTe. This maximum is based on the assumption that 100% of the photons are absorbed by nc-CdTe and that 100% of the electrons generated are transferred to the H_2ase^A, with a maximum of two photons per molecule of H_2. The total measured output of H_2 was 10.2 ± 1.1 nmol, which is a photon-to-H_2 conversion efficiency of 9.0 ± 1.0%. This is likely to be a lower limit of the conversion efficiency, as it is the average for the entire distribution of molecular complexes in a 2:1 mixture. In view of the results in Figures 4 and 7, it is possible that a homogeneous distribution of complexes might yield a higher efficiency. The white-light efficiency at AM 1.5 (6.64 mmol of photons s^{-1} m^{-2})[49] was also calculated by this method and found to be 1.8 ± 0.2%.

Conclusions

The results presented here demonstrate that controlled self-assembly of MPA-capped nc-CdTe and H_2ase^A can form stable charge-transfer complexes capable of catalyzing light-driven H_2 production with a single-wavelength quantum yield of 9% and an AM 1.5 efficiency of 1.8%. The observed TON of H_2 production under illumination was 25 mol H_2 mol^{-1} H_2ase s^{-1}, and compares well to the values recently published for light-driven H_2 production by other H_2ase hybrid complexes. For example, when the [NiFeSe]-H_2ase from *Desulfomicrobium baculatum* was adsorbed onto dye-sensitized TiO_2,[10,11] a TON of 50 mol H_2 mol^{-1} H_2ase s^{-1} was observed. Immobilization of the membrane-bound [NiFe]-H_2ase from *Ralstonia eutropha* fused to photosystem I (PSI) on a Au electrode resulted in a TON under an applied potential (−90 mV) of 75 mol H_2 mol^{-1} H_2ase s^{-1}.[57] More recently, the *C. acetobutylicum* H_2ase investigated in this study was physically wired to PSI, which in solution resulted in a TON of ∼0.14 mol H_2 mol^{-1} H_2ase s^{-1}.[58]

In this study, the H_2 production TON for nc-CdTe-H_2ase was maximal for complexes that were formed at lower H_2ase ratios (see Figure 7). Orientation within these complexes was controlled by the selection of MPA as the capping ligand on nc-CdTe, to result in a compatible surface charge with H_2ase and docking of nc-CdTe adjacent to the surface-localized distal [4Fe−4S] cluster. This predicted arrangement is consistent with the effect of solution ionic strength on complex self-assembly

(47) Matylitsky, V. V.; Dworak, L.; Breus, V. V.; Basche, T.; Wachtveitl, J. *J. Am. Chem. Soc.* **2009**, *131*, 2424–2425.
(48) Trinh, M. T.; Houtepen, A. J.; Schins, J. M.; Hanrath, T.; Piris, J.; Knulst, W.; Goossens, A. P. L. M.; Siebbeles, L. D. A. *Nano Lett.* **2008**, *8*, 1713–1718.
(49) Noy, D.; Moser, C. C.; Dutton, P. L. *Biochim. Biophys. Acta* **2006**, *1757*, 90–105.
(50) Humphrey, W.; Dalke, A.; Schulten, K. *J. Mol. Graphics* **1996**, *14*, 33–38.
(51) Stone, J. *An Efficient Library for Parallel Ray Tracing and Animation*; University of Missouri-Rolla: Rolla, MO, 1998.
(52) Pandey, A. S.; Harris, T. V.; Giles, L. J.; Peters, J. W.; Szilagyi, R. K. *J. Am. Chem. Soc.* **2008**, *130*, 4533–4540.
(53) Comeau, S. R.; Gatchell, D. W.; Vajda, S.; Camacho, C. J. *Nucleic Acids Res.* **2004**, *32* (Suppl. 2), W96–W99.
(54) Comeau, S. R.; Gatchell, D. W.; Vajda, S.; Camacho, C. J. *Bioinformatics* **2004**, *20*, 45–50.
(55) Comeau, S. R.; Kozakov, D.; Brenke, R.; Shen, Y.; Beglov, D.; Vajda, S. *Proteins* **2007**, *69*, 781–785.
(56) Kozakov, D.; Brenke, R.; Comeau, S. R.; Vajda, S. *Proteins* **2006**, *65*, 392–406.
(57) Krassen, H.; Schwarze, A.; Friedrich, B.; Ataka, K.; Lenz, O.; Heberle, J. *ACS Nano* **2009**, *3*, 4055–4061.
(58) Lubner, C. E.; Grimme, R.; Bryant, D. A.; Golbeck, J. H. *Biochemistry* **2010**, *49*, 404–414.

and stability. Both PL bleaching and light driven H_2 production were evidence of ET between the nc-CdTe and surface-bound H_2ase^A, with k_{ET} being competitive with intrinsic charge recombination pathways in nc-CdTe. Light-driven H_2 production required the presence of ascorbic acid as a hole scavenger, and efficiencies were dependent on the ascorbic acid concentration. In addition, the luminescent properties of nc-CdTe were found to influence photocatalysis, where a higher PLQE supported higher rates of H_2 production. This strongly suggests that photogenerated electrons are transferred out of nc-CdTe core states, not surface traps, to the H_2ase^A. The relative contribution of ET to nc-CdTe relaxation was strongly affected by the nc-CdTe-H_2ase^A molar ratio, with lower H_2ase^A surface coverages resulting in a larger contribution of ET and higher H_2 production rates. A global effect of nc-CdTe-H_2ase^A stoichiometry on the photocatalytic properties of hybrids demonstrates the importance of the assembly process to obtaining optimal molecular architectures. The contribution of the ET and hole scavenging reaction kinetics to the overall kinetics of light-driven H_2 production in nc-CdTe-H_2ase remains to be determined. However, H_2 production rates were dependent on ascorbic acid concentration (hole scavenging) and on nc-CdTe-H_2ase ratio (ET), suggesting that either of these transfer steps can potentially be rate limiting. Characterization of the kinetic parameters along with modifications in the nanocrystal composition, size, and capping group and limitation of ensemble distributions to achieve more uniform architectures should provide insight into how conversion efficiencies can be improved.

Acknowledgment. This research was funded by the Photo- and Bio- Chemistry Programs of the Chemical Sciences, Geosciences, and Biosciences Division, Office of Basic Energy Sciences, Office of Science, U.S. Department of Energy. We also thank John Baker for his valuable assistance with PL measurements and Jeffery Blackburn, Drazenka Svedruzic, Maria L. Ghirardi, and Qing Song for their valuable comments and helpful discussions.

Supporting Information Available: White-light spectra, Langmuir fit values and plots, and the derivation of eq 8. This material is available free of charge via the Internet at http://pubs.acs.org.

JA101031R